Preliminary analysis of effect of random segment errors on coronagraph performance

Mark T. Stahl[a], Stuart B. Shaklan[b], and H. Philip Stahl[a]
[a]NASA Marshall Space Flight Center;
[b]Jet Propulsion Laboratory, California Institute of Technology.

ABSTRACT

Are we alone in the Universe is probably the most compelling science question of our generation. To answer it requires a large aperture telescope with extreme wavefront stability. To image and characterize Earth-like planets requires the ability to block 10^{10} of the host star's light with a 10^{-11} stability. For an internal coronagraph, this requires correcting wavefront errors and keeping that correction stable to a few picometers rms for the duration of the science observation. This requirement places severe specifications upon the performance of the observatory, telescope and primary mirror. A key task of the AMTD project (initiated in FY12) is to define telescope level specifications traceable to science requirements and flow those specifications to the primary mirror. From a systems perspective, probably the most important question is: What is the telescope wavefront stability specification? Previously, we suggested this specification should be 10 picometers per 10 minutes; considered issues of how this specification relates to architecture, i.e. monolithic or segmented primary mirror; and asked whether it was better to have few or many segmented. This paper reviews the 10 picometers per 10 minutes specification; provides analysis related to the application of this specification to segmented apertures; and suggests that a 3 or 4 ring segmented aperture is more sensitive to segment rigid body motion that an aperture with fewer or more segments.

Keywords: Space Telescope Mirrors, Segmented Mirrors, Systems Engineering, Conoragraph

1. INTRODUCTION

Per the NRC ASTRO2010 Decadal Survey[1]: "One of the fastest growing and most exciting fields in astrophysics is the study of planets beyond our solar system. The ultimate goal is to image rocky planets that lie in the habitable zone of nearby." Per the NRC 2012 report 'NASA Space Technology Roadmaps & Prioroties'[2], the second highest technical challenge for NASA regarding expanding our understanding of Earth and the universe in which we live is "Develop a new generation of astronomical telescopes that enable discovery of habitable planets, facilitate advances in solar physics, and enable the study of faint structures around bright objects by developing high-contrast imaging and spectroscopic technologies to provide unprecedented sensitivity, field of view, and spectroscopy of faint objects." NASA's 2014 Astrophysics Plan 'Enduring Quests Daring Visions'[3] recommended building an 8 to 16-meter Large UV/Optical/Infrared (LUVOIR) Surveyor mission with sufficient sensitivity and angular resolution to "dramatically enhance detection of Earth-sized planets to statistically significant numbers, and allow in-depth spectroscopic characterization. Finally, AURA's 2015 report 'Cosmic Birth to Living Earths'[4] states that "a 12 meter class space telescope with sufficient stability and appropriate instrumentation can find and characterize dozens of Earth-like planets and make transformational advances in astrophysics".

To directly image and characterize Earth-like habitable-zone planets requires the ability to block 10^{10} of the host star's light. This can be done with either an external star shade or an internal coronagraph. For an internal coronagraph, diffraction effects from the telescope aperture and wavefront errors in the telescope causes the stellar light to scatter about the occulting mask and introduces noise. Sources of these errors can be rigid-body misalignments between the optical components, mounting error or low-order and mid-spatial frequency figure errors of the optical components themselves. For example, a lateral misalignment between the primary and secondary mirror introduces coma into the wavefront. If the errors are static, it is possible to correct them via Wavefront Sensing and Control (WFSC) and Deformable Mirrors (DMs) – limited by the number of DM actuator spatial frequency. Or, they can be removed via calibration and subtraction.

But, it is not sufficient to simply block this light, it is necessary to block this light with a 10^{-11} 'instantaneous' stability (not averaged over science integration time because intensity does not average to zero) to provide an adequate signal to noise ratio.[5] For an internal coronagraph, this requires correcting wavefront errors and keeping that correction stable to a

few picometers rms for the duration of the science observation. This science requirement places severe specifications upon the performance of the integrated observatory, telescope and primary mirror.

The Advance Mirror Technology Development (AMTD) project was initiated in FY12 to mature by at least a half TRL critical technologies required to enable 4 to 8 meter UVOIR space telescope primary mirror assemblies for both general astrophysics and ultra-high contrast observations of exoplanets. AMTD uses a science-driven systems engineering approach. We mature technologies required to enable the highest priority science AND result in a high-performance low-cost low-risk system. A key task is to define telescope level specifications traceable to science requirements and flow those specifications to the primary mirror. The purpose of AMTD is not to design a specific telescope for a specific mission. We are not producing an optical design or prescription. We are producing a set of engineering specifications which will enable the on-orbit telescope performance required to enable the desired science. Our philosophy is to define a set of specifications which 'envelop' the most demanding requirements of all potential science. From a systems perspective, probably the most important question is: What is the telescope wavefront stability specification? This specification will be a primary driver on telescope design, including: primary mirror support structure stiffness, secondary mirror structure stiffness, passive & active vibration isolation, and passive & active thermal control.

Previously, we have suggested that this specification should be < 10 picometers per 10 minutes; considered issues of how this specification relates to architecture, i.e. monolithic or segmented primary mirror; and asked (without providing an answer) whether it was better to have few or many segments.[6, 7] An initial answer to this question was provided by Dr. Shaklan at NASA's Mirror Technology Days.[8] This paper reviews the < 10 pm per 10 min specification; provides analysis related to the application of this specification to segmented apertures; and suggests that a 3 or 4 ring segmented aperture is more sensitive to segment rigid body motion that an aperture with fewer or more segments.

2. TELESCOPE WAVEFRONT STABILITY SPECIFCATION

Independent of telescope architecture needed to provide 'sufficient' sensitivity and angular resolution, the most important capability required to enable direct characterization of a habitable-zone Earth-sized planet is the ability to block 10^{10} of the host star's light and create a 'dark hole' with 10^{-11} contrast stability. To perform 10^{-11} contrast stable science, using an internal coronagraph, requires an ability to correct wavefront errors to picometer levels and maintain that level of correction over the duration of the science observation. If these errors are slow (i.e. mechanical slippage or thermal drift), it is assumed that the coronagraph's wavefront sensing and control system (WFSC) and deformable mirrors (DMs) can correct the error. But, if the errors fast (i.e. caused by mechanical vibration), then the light leakage produces an average contrast noise floor. Such a science requirement places severe, never previously attempted or demonstrated, specifications upon the performance of the integrated observatory, telescope and primary mirror, including: primary mirror support structure stiffness, secondary mirror structure stiffness, passive & active vibration isolation, and passive & active thermal control. But, what exactly is the required telescope stability specification?

Green and Shaklan (2003)[9] state that picometer level wavefront control is needed to achieve and maintain stability. They analyzed the sensitivity of candidate coronagraph designs to linearly increasing amounts of low-order aberrations (tilt, focus, astigmatism, coma, trefoil and spherical). Each design has its own aberration sensitivities. All studied designs were most sensitive to spherical but sensitivity to the other aberrations varied. And sensitivities vary with angular separation from the central core. Additionally, they derived a maximum observation time based on specifics of the coronagraph design and the rate at which the telescope wavefront error increases. Beyond this time, speckle noise will obscure the exoplanet signal. To enable very long science exposures (because the exoplanet is faint), the telescope wavefront error must be very stable (on the order of a few picometers) during the entire duration of the desired science exposure. A key systems issue identified is the impact of how fast the wavefront error changes on the ratio of science exposure time to wavefront control overhead.

Shaklan, et al (2011)[10] provides a detailed stability error budget for a 3.8 meter telescope coupled with a band-limited coronagraph. For this coronagraph, coma is the most important aberration and to maintain the required contrast stability, rigid body alignment between the primary and secondary mirror need to be controlled to the 1 to 8 picometer level depending on exact dimensional parameter and desired λ/D inner working angle (IWA) (tolerances are more relaxed at 3λ/D than at 2λ/D). This is an important point. They report that at an IWA of 2.5 λ/D the requirements are relaxed by a factor of 2 relative to an IWA of 2 λ/D. And, at 3 λ/D the requirements are relaxed by a factor of 4 relative to 2 λ/D. It is necessary to maintain this level of alignment for periods of minutes to days. However, it is possible to relax these stability requirement by approximately an order of magnitude by using WFSC and DMs to actively correct for slowly

varying low-order errors. The most important contribution of this and other similar papers is to define the maximum allowed residual error budget for an actively corrected telescope as a function of IWA.

Analysis of wavefront stability as a function of IWA is important because it allows one to derive an engineering specification from a science requirement. The AURA 2015 report[4] calls for a 12 meter class space telescope. But, the real requirement is to do 10^{-10} contrast science at 40 milli-arc-seconds at a wavelength of 800 nm. This can be accomplished with an 8-m telescope operating at an IWA of 2 λ/D. Or, it can be done at 3 λ/D with a 12-m telescope (Table 1). Where this becomes interesting is if the required WFE stability at 3 λ/D is 4X larger than at 2 λ/D – because, to first order, a 12-m mirror is only 2.25X less stiff than an 8-m mirror. Thus, theoretically, it may be easier to achieve 4 pm rms with a 12-m aperture than to achieve 1 pm rms with an 8-m aperture.

Table 1: Notional WFE Stability versus IWA as function of Aperture Size

	Inner Working Angle				
	λ/D	2 λ/D	2.5 λ/D	3 λ/D	4 λ/D
Stability [pm rms]		1	2	4	
Aperture [m]	Inner Working Angle at 800 nm [mas]				
4	40	80	100	120	160
8	20	40	50	60	80
12	14	28	35	41	55

Lyon and Clampin (2012)[11] provides a methodology for calculating temporal stability requirements. They calculate the time needed to yield a SNR = 5 for a 20% spectral band at 550nm at an IWA = 2λ/D for each star in the Hipparcos (HIP30) database of 2350 stars out to 30 parsecs. Their SNR calculation includes: photon noise from stellar light leakage (speckle noise), the planet, Zodi and exoZodi. Telescope WFE stability and exposure times varies as a function of which star is being investigated. For G-class stars the exposure time varies by approximately two orders of magnitude. The length of the exposure scales with telescope diameter to $\sim D^{10/3}$. For a 4-m telescope SNR=5 exposure time varies from 1000 to 100,000 seconds (16 min to 27 hours). For an 8-m class telescope the time varies from 100 to 10,000 seconds (1.6 min to 2.7 hours). Regarding WFE stability, they specify their entrance pupil wavefront using a spatial-temporal PSD (power spectral density) because a WFE at a given spatial frequency produces a speckle (whose size is determined by the Lyot stop diameter) at the same spatial frequency. For a 4-m class telescope, they find that the most stressing requirement is a wavefront tolerance on the order of 8 pm rms. The requirement is a strong function of IWA and for most G-stars is larger than 8 pm rms. An important contribution of this paper is its discussion of control period versus WFE drift period. The time to sense and control is limited by photon statistics which sets a bound on recovery of wavefront errors based on the photon count rates. They calculate that the WFSC system needs ~200,000 'detected' photons per speckle (spatial frequency) to control the wavefront to 100 pm and that, to maintain this level of precision, the WFSC control frequency needs to be 4 to 10 times faster than the drift frequency. They provide an equation which can be rearranged to solve for WFSC integration period as a function of control accuracy and detected photon rate:

$$T_{integration} = (\lambda/4\pi)^2 \, (1/\sigma_{WFE})^2 \, (1/\text{Detected Photon Rate})$$

Assuming a constant detected photon rate, controlling to 1 pm requires 10,000 longer integration time than to 100 pm. Alternatively, controlling to 1 pm rms requires ~2 x 10^9 detected photons. A fundamental consequence of requiring so many detected photons is that WFSC approaches based only on leaked starlight, without modulating to increase the counts, have prohibitively long sensing times. Approaches that use all the stellar photons have sensing times that are about eight orders of magnitude shorter than schemes that use only leaked photons. While not discussed in the paper, one might draw an inference that the 10 picometer rms stability requirement is for each spatial frequency in the PSD. All examples are for single PSD spatial frequencies.

Krist, et. al. (2012)[5] performed a point design for a 4-m telescope looking at a V=5 magnitude star. They calculated that a low order wavefront sensor (first 11 Zernikes) could accurately measure WFE changes of 5 to 8 pm rms at a cadence of 60 to 120 seconds. This analysis assumes that the WFSC system is using photons reflected off of the occulting mask over a 500 to 600 nm pass band. If one invokes a 10X control versus drift period, then this WFSC system can correct for a WFE drift of ~10 pm per 10 to 20 minutes. Given that control accuracy scales with the square root of exposure time or telescope area, the allowable wavefront drift for an 8-m telescope would be ~10 pm per 2.5 to 5 minutes.

However, the AURA report[4] also calls for the characterization of dozens of candidate exoEarths. And to accomplish this goal will required investigating stars that are dimmer than V=5. Figure 1 shows a distribution of apparent stellar V magnitude for the target list that maximizes exoEarth yield for an 8-m telescope, as determined from a DRM simulation

by Chris Stark (private communication). This simulation uses the methodology described by Stark et. al. (2015)[12] for an 8-m aperture operating at a 3λ/D IWA; SNR=10, R=70 V-band spectrum for each detected exoEarth; and eta_Earth=0.2. Given that the most exoEarths are expected to be around V=6 stars, the Telescope/WFSC system must be designed to operate for V=6 stars. Thus, because a V=6 star has 2.5 fewer photons than a V=5 star, the telescope stability period must be 2.5 times longer than what is calculated for a V=5 star.

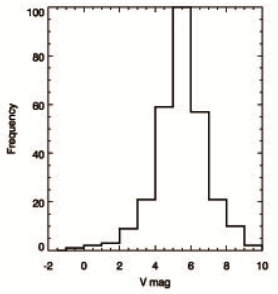

Fig 1: Host Star Magnitudes

Thus far, we have reviewed only the wavefront stability specification for monolithic aperture telescopes. But, the AURA report[4] calls for a 12 meter class space telescope. The only way to achieve this is via segmenting the primary mirror. As discussed in Appendix A, there are many different segmentation schemes and each produces its own characteristic point spread function. Diffraction moves energy from the PSF core into side-lobe peaks – some of which may be in the 'dark-hole'. The amount of energy that gets moved depends on the size of gaps between segments and segment 'phasing' (where 'phasing' is rigid body alignment of the segments relative to a common surface). Ideally, segmented deformable mirrors and clever coronagraph design can mitigate gaps size and alignment issues, but dynamic segment motion is a problem. Segment 'rocking' will cause the diffraction spikes to 'wink'. Co-phasing (or piston) produces speckle noise – where the size of these speckles is determined by segment size.

Per Guyon (2012)[13], uncorrelated co-phasing errors produce a speckle halo that effects contrast between the coronagraph's IWA and the diffraction limit of a single segment (which is potentially a reason for larger segments); and, this effect is independent of coronagraph concept. Also, for active control, segment drift period should be ~10X slower than the WFSC sampling rate. As summarized in Table 2, the co-phasing specification required to achieve a given contrast level depends only on the total number of segments and is independent of telescope diameter. The more segments; the more relaxed the co-phasing specification. And, the time required to control co-phasing (for a given magnitude star) depends only on telescope diameter, i.e. is independent of the number of segments. The larger the telescope diameter; the faster the control. The reason is: while it takes longer to measure a smaller segment's co-phasing error because there are fewer photons, it takes less time to measure the larger error allowed by having more segments.

Table 2: Segment co-phasing requirements for ideal space-based telescopes[13]
(wavefront sensing done at λ=550nm with an effective spectral bandwidth δλ= 100 nm)

Telescope diameter (D) & λ	Number of Segments (N)	Contrast	Target	Cophasing requirement	Stability timescale
4 m, 0.55 μm	10	1e-10	m_V=5	2.8 pm	13.3 min
8 m, 0.55 μm	10	1e-10	m_V=5	2.8 pm	3.3 min
8 m, 0.55 μm	100	1e-10	m_V=5	8.7 pm	3.3 min

Measuring a single sine wave to 0.8 pm amplitude on a Magnitude V=5 star with an 8-m diameter telescope and a 100 nm effective bandwidth takes 20 seconds. A single WFSC measurement of the primary mirror requires 10^{11} 'incident' photons and V=5 star has 10^6 photons/m2-sec-nm. But, controllability needs 10 measurements, thus stability period requirement is 200 seconds or 3.3 minutes. This result is not exactly the same as the Krist result, but it is within a factor of 2. And, for a V=6 star, the Guyon stability time for an 8-m telescope would be 8.3 minutes.

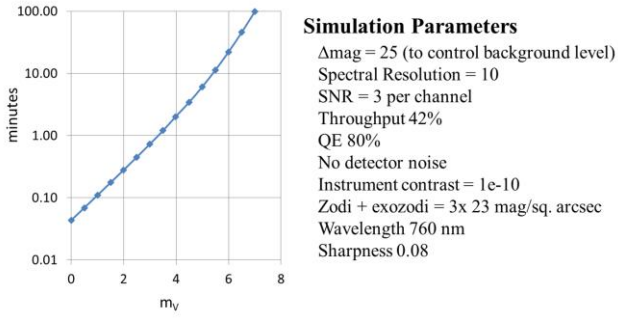

Figure 1: Wavefront Stability Specification for a 10-meter telescope with a nominal Coronagraph.

Shaklan (2014)[8] calculated the stability time for a 10 meter telescope with a nominal coronagraph operating at 760 nm. Given that the majority of exoEarths are expected around Magnitude 5 and 6 host stars, the telescope must maintain picometer WFE stability for approximately 20 minute periods. This period can be shortened by operating at 550 nm.

In summary:

- Independent of telescope aperture size or architecture (monolithic or segmented) and coronagraph design, to achieve 10^{-11} contrast stability requires a wavefront that is stable to better than 10 picometers rms. The exact WFE stability is a function of desired coronagraph inner working angle.

- Per Lyon and Clampin: WFSC time is limited by photon statistics. To control to 1 pm rms, the WFSC system needs requires ~2 x 10^9 'detected' photons. And, to maintain this level of precision, the WFSC control frequency needs to be 4 to 10 times faster than the drift frequency.
- Per Guyon: The WFSC system needs ~10^{11} 'incident' photons per spatial frequency to control the wavefront to 0.8 pm amplitude. And, the telescope needs to be stable for a period 10X longer than the WFSC control period.
- Assuming a nominal WFSC architecture using rejected light from the coronagraph occulting mask, the length of time for which the telescope must maintain < 10 picometer rms wavefront stability depends on aperture size and star magnitude. Table 3 illustrates this scaling relationship for a nominal assumed WFSC system.

Table 3: WFSC Period and Telescope Stability Period as a function of Aperture Size and Star Magnitude

	V = 5		V = 6		V = 7	
Aperture [m]	T_{WFSC} [min]	$T_{WFE\ Stability}$ [min]	T_{WFSC} [min]	$T_{WFE\ Stability}$ [min]	T_{WFSC} [min]	$T_{WFE\ Stability}$ [min]
4	2	20	5	50	12.5	125
8	0.5	5	1.25	12.5	3	30
12	0.25	2.5	0.625	6.25	1.5	15

- A telescope wavefront stability specification of < 10 picometers rms per 10 minutes may not be sufficient, but it continues to be a 'good' placeholder specification.

The only way to get a better specification is to perform detailed systems engineering trade studies. Start with the science requirement (10^{-11} contrast stability at 40 mas at 800 nm) and determine the sensitivity of each candidate coronagraph design to wavefront error instability. Then calculate the WFSC control integration time required for the dimmest stars to be investigated. The telescope stability period must be 10X longer than the WFSC control time. It is important to note that if WFSC is occurring in series with science, then it is going to have a significant impact on observing efficiency. In fact, there may be a cut-off on how dim of a star can be searched for an Earth-like planet in the Habitable Zone.

Finally, this is an engineering performance specification. How such a specification might be accomplished is beyond the scope of this paper. Appendix B presents examples of the state of the art and implementation factors of how space telescopes respond to mechanical and thermal stimuli.

3. SEGMENTED TELESCOPE WAVEFRONT STABILITY

At the end of Stahl, et. al. (2013)[6] we asked if it is it better to have fewer large segments or many small segments. Shaklan[8] did a preliminary analysis to convert the science stability requirement into an engineering specification. He created a simple Matlab© model of a 10-m square aperture telescope with 2×2, 4×4, and 8×8 grid of square segments and calculated the contrast leakage produced by 1-nm rms random piston and 1-nm rms random tilt errors as a function of segmentation. For an 8×8 aperture, the contrast stability is >10^{-7}. To achieve a contrast stability of <10^{-11} requires that the rms error must be <10 pm. But, for a 2x2 aperture, the maximum allowed rms WFE is ~50 pm rms.

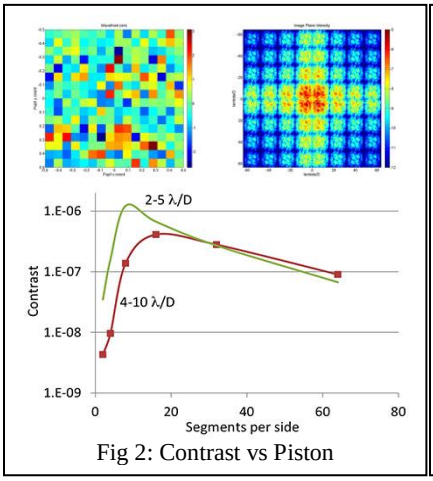

Fig 2: Contrast vs Piston

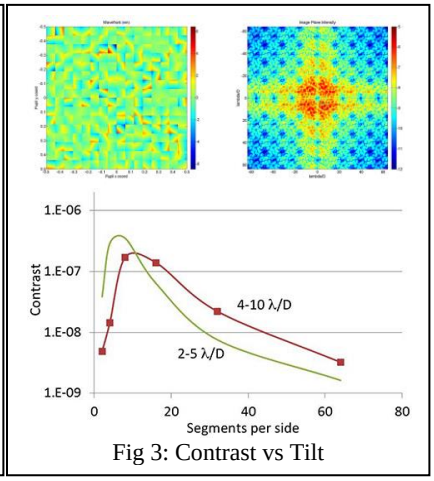

Fig 3: Contrast vs Tilt

Starting with Dr. Shaklan's preliminary Matlab© model, we have rewritten and generalized the code and expanded it to include hexagonal segments. The model is consistent with Sivaramakrishnan[20] and Soummer[21] and currently uses an X- & Y-1D 4th order band-limited coronagraph mask (Kuchner & Traub, 2007[22]). The tool input is a pupil function

$$\text{Pupil}(x,y) = \text{Aperture}(x,y) * \text{Phase}(x,y) = A(x,y)e^{i\Phi(x,y)}$$

The aperture function uses 512 x 512 pixels and $\gamma = 6$ zero padding to define the input wavefront boundary. Currently, the tool can model monolithic or segmented apertures with circular, hexagonal or square outer boundary shape. Segments can be hexagonal, petals around a center segment, or square. Currently, the tool can model up to 6 rings of hexagonal segments or up to 512 x 512 square segments. The tool can place integer number of pixel 'gaps' between segments – but we are not using this capability for this analysis. And, the tool can impose central obscurations and secondary mirror spiders – but again, we are not using this capability for this analysis.

At present, the tool models in the phase function random rigid body errors (i.e. piston and tilt) for continuous mirror elements, i.e. monolith or segments. The reason for random errors is that we assume there is a WFSC system that is able to measure and correct static wavefront error. But, that this system is not able to correct for random fluctuations. In the future we plan to include correlated tilt error, because as discussed in Appendix B, segment 'rocking-mode' error can be a significant problem for segmented apertures. Additionally, we plan to add Siedel aberrations such as coma (motion between primary and secondary mirror) and astigmatism (primary mirror support structure 'wing flap').

We used this model to explore how random rigid body motion effects contrast leakage as a function of aperture segmentation. For this study we defined 6 aperture segmentation architectures (Figure 4): monolithic, center segment surrounded by a ring of half height segments (which we call the half ring architecture); and a center segment surrounded by 1, 2, 3 or 4 rings of full size segments (i.e. same size as center segment). On each aperture architecture we imposed random piston and tilt errors of amplitude 1.0 nm, 100 pm and 10 pm and measured the contrast as a function of angular separation in the focal plane.

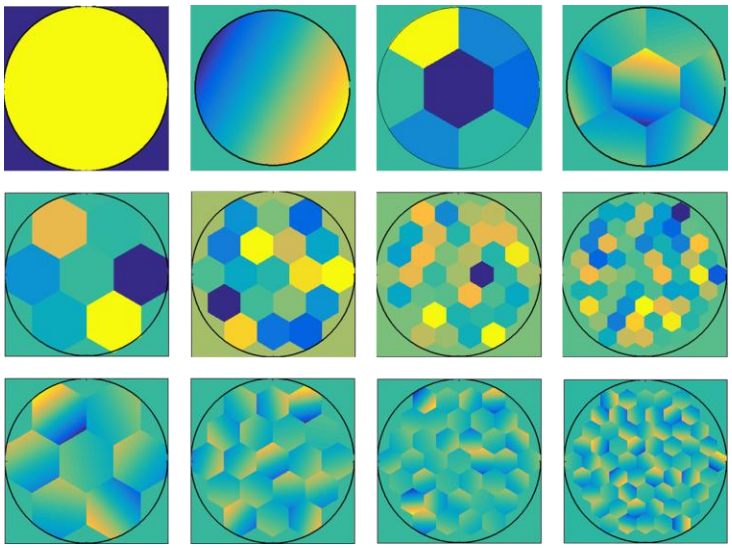

Figure 4: Aperture Segmentations Architectures used in Contrast Leakage Study

For each segmentation architecture, multiple realizations (typically 16) were calculated and averaged. Figure 5 (a) shows for a 1-ring hex aperture the input pupil function for random piston; 5(b) shows a single contrast realization for this pupil function and 5(c) shows the average of 16 realizations. The boxes in 5(b) define regions of interest over which average contrast is calculated for Figure 8: 1x1 from 1 to 2 λ/D; 3x3 from 2 to 5 λ/D; and 6x6 from 4 to 10 λ/D. The bottom right 5(d) shows profiles of contrast leakage versus angular separation (λ/D) for three different 16 averages: random piston error of 1 nm rms, 100 pm rms and 10 pm rms. The line in 5(c) shows where the profile slice is extracted from the 16-averge result. The error bars in 5(d) and Figure 7 show the PV range of contrast leakage for each of the 16 realizations. There is significant variation from run to run. Figure 6(a) shows profile plots of 16 individual realizations for a 1 ring hex system with 10 pm rms random piston error and Figure 6(b) shows five different 50 average runs. Figure 7 shows the piston and tilt results for each of the aperture segmentation architectures.

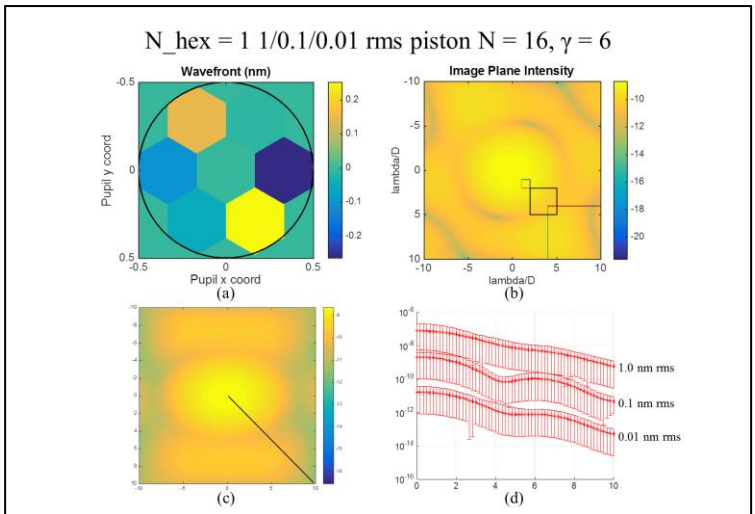

Fig 5: (a) Input Pupil Function; (b) Single Realization Contrast Output with Region of Interest Boxes; (c) 16 Average Contrast Output with Profile Slice; (c) 3 profiles for 1.0 nm, 100 pm and 10 pm rms error.

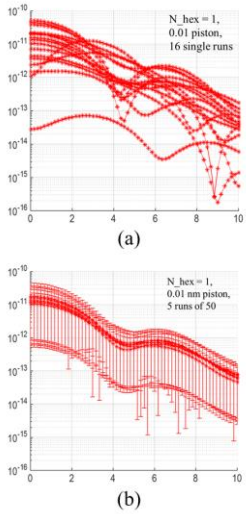

Fig 6: (a) variability of single runs; (b) variability of 50 averages

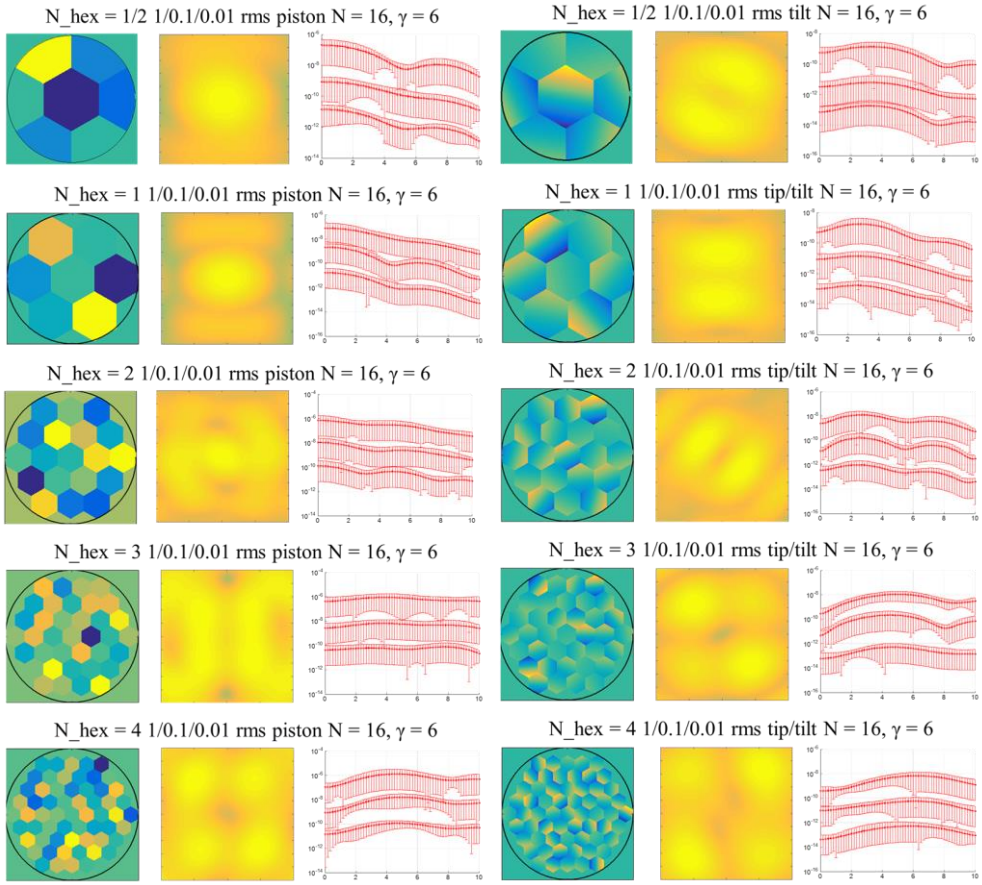

Fig 7: Summary Plot of Segmented Aperture Contrast Sensitivity to Random Piston & Tilt Errors

Please note in Figure 7 how it illustrates the relationship between segmentation spatial frequency and where energy is moved from the central core. Also, a 10X change in stability results in a 100X change in contrast leakage.

To answer the question as to whether it is better to have fewer or more segments, the average contrast leakage was calculated for each architecture over the 3 regions of interest (1 to 2 λ/D, 2 to 5 λ/D, and 4 to 10 λ/D) for random piston and tilt error (Figure 8). In general, for every region of interest, it is better to have fewer segments. The worst configurations in our analysis were those with 2 to 4 rings. As expected from Shaklan (2011)[10], at larger angles from the PSF core, contrast leakage was less sensitivity to piston and tilt error. Thus, a segmented observatory using an internal coronagraph operating at 4 λ/D can tolerate more piston and tilt error than the same observatory operating at 2 λ/D or 3 λ/D. Finally, our model was 10X less sensitive to tilt error than to piston error. All of these findings are consistent with the Shaklan[8] preliminary analysis using square segments in a square aperture (Figures 2 and 3).

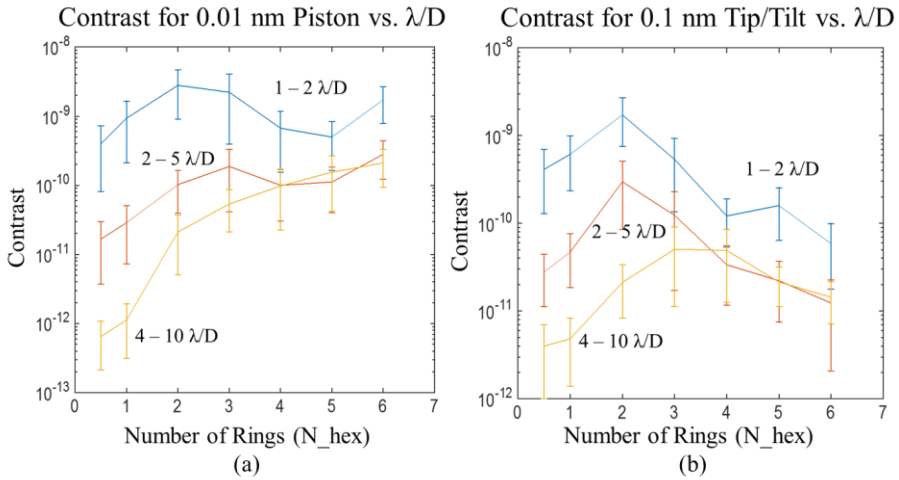

Fig 8: Contrast Leakage as a function of Number of Segments per Radius for (a) Piston and (b) Tilt.
Note: (1) fewer segments are better and (2) contrast is 10X less sensitivity to Tilt error than to Piston Error

4. CONCLUSIONS

The Advance Mirror Technology Development (AMTD) project was initiated in FY12 to mature by at least a half TRL critical technologies required to enable 4 to 8 meter UVOIR space telescope primary mirror assemblies for both general astrophysics and ultra-high contrast observations of exoplanets. AMTD uses a science-driven systems engineering approach. A key task is to define telescope level specifications traceable to science requirements and flow those specifications to the primary mirror. Probably the most important specification to define is telescope wavefront stability. Wavefront stability will be a primary driver on telescope design, including: primary mirror support structure stiffness, secondary mirror structure stiffness, passive & active vibration isolation, and passive & active thermal control.

A proper specification requires a detailed systems engineering trade studies. Start with the science requirement (10^{-11} contrast stability at 40 mas at 800 nm) and determine the sensitivity of each candidate coronagraph design to wavefront error instability. Then calculate the WFSC control integration time required for the dimmest stars to be investigated. The telescope stability period must be 10X longer than the WFSC control time. It is important to note that if WFSC is occurring in series with science, then it is going to have a significant impact on observing efficiency. In fact, there may be a cut-off on how dim of a star can be searched for an Earth-like planet in the Habitable Zone.

But, to first order, wavefront stability is independent of telescope aperture and coronagraph design. It does, however, depend on aberration type and IWA. Green and Shaklan (2003)[9] and Shaklan (2011)[10] show how stability error budget varies for different low order aberrations. And, Figure 8 shows that there may be a 10X difference in sensitivity between piston and tilt for a segmented system. Regarding IWA, Shaklan (2011)[10] asserts that that the wavefront stability requirement is 4X smaller at 2 λ/D than at 3 λ/D. Figure 8 shows that stability for segmented systems is also relaxed at larger λ/D. An interesting design question is whether a larger aperture is better than a smaller aperture. Since the science requirement is 40 mas, this can be achieved at 2 λ/D with an 8-m telescope or 3 λ/D with a 12-m telescope. Now, of course it costs more to make a 12-m telescope than it costs to make an 8-m telescope, but the real question is: does it cost more to make a 12-m telescope with 20 pm rms stability or an 8-m telescope with 5 pm rms stability.

Regarding the Wavefront Stability Specification, we have answered half of the question. The amplitude is very small and extremely challenging, i.e. on the order of a few picometers to 10s of picometers and if we are really lucky – maybe as much as 100 pm rms for some error forms.

But, for what length of time must the telescope be this stable? Rearranging an equation from Lyon and Clampin (2012)[11] provides the WFSC integration period as a function of control accuracy and detected photon rate:

$$T_{integration} = (\lambda/4\pi)^2 \, (1/\sigma_{WFE})^2 \, (1/\text{Detected Photon Rate})$$

The period over which the telescope must be stable depends on the accuracy to which the wavefront stability must be controlled and detected photon rate. Assuming a constant detected photon rate, controlling to 1 pm requires 100 longer integration time than to 10 pm. This can have a significant impact on the required stiffness for a given telescope. Regarding detected photon rate, this depends on the size of the telescope aperture and the magnitude of the star being investigated. Controlling with a V=6 star takes 2.5 times longer than with a V=5 star. Table 3 summarized these findings for a nominal assumed WFSC system. Also, Lyon and Clampin (2012)[11] provide a formal argument as to why the telescope must be stable for a period 10X longer than the control time.

Table 3: WFSC Period and Telescope Stability Period as a function of Aperture Size and Star Magnitude

	V = 5		V = 6		V = 7	
Aperture [m]	T_{WFSC} [min]	$T_{WFE\ Stability}$ [min]	T_{WFSC} [min]	$T_{WFE\ Stability}$ [min]	T_{WFSC} [min]	$T_{WFE\ Stability}$ [min]
4	2	20	5	50	12.5	125
8	0.5	5	1.25	12.5	3	30
12	0.25	2.5	0.625	6.25	1.5	15

Thus, while not perfect or even exactly correct because of things such as sensitivity to IWA and sensitivity to star contrast or spectral band, a wavefront stability specification of < 10 pm rms per 10 minutes is a good first order bounding specification.

Finally, to answer the question as to whether it is better to have fewer or more segments, we studied 7 different aperture segmentation architectures: center segment surrounded by a ring of half height segments (which we call the half ring architecture); and a center segment surrounded by 1, 2, 3, 4, 5 and 6 rings of full size segments (i.e. same size as center segment). We used an analytical model to calculate each architecture's contrast leakage sensitivity to random piston and tilt errors over the 3 regions of interest (1 to 2 λ/D, 2 to 5 λ/D, and 4 to 10 λ/D). As shown in Figure 8, for every region of interest, it is better to have fewer segments. The worst configurations in our analysis were those with 2 to 4 rings.

APPENDIX A: SEGMENTED APERTURE POINT SPREAD FUNCTION

There are many segmentation schemes, ranging from hexagonal segments to pie segments to multiple large circular mirrors. Each with its own characteristic point spread function (PSF). From Yaitskova et al (2003),[14] Figure A-1 shows an aperture composed of hexagonal segments and its resultant PSF; where a PSF of a telescope is found by taking the Fourier transform of its aperture function. For a hexagonal segmented telescope, the aperture function is described by a hexagonal segment convolved with a grid(r) function. If one assumes that the segments are all identical (which in practice they are not) and that the grid function is regular (which in practice it is not), then the telescope PSF is described by the product of the PSF for the segments and the Grid(ρ) function (Fourier transform of the grid(r) function).

$$PSF_{tel} \sim PSF_{seg}\ Grid(\rho) \sim \mathcal{F}\{\text{segment } ** \text{ grid(r)}\}$$

where: PSF_{tel} diameter $\sim \lambda/D_{tel}$ PSF_{seg} diameter $\sim \lambda/d_{seg}$ Grid space $\sim \lambda/d_{seg}$

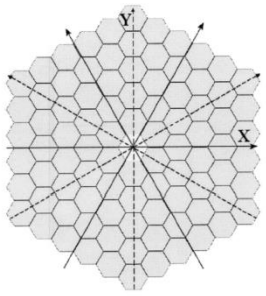

Fig. 1. Segmented mirror with segmentation order $M = 5$ consisting of $N = 90$ segments. Solid and dashed arrows illustrate the double $\pi/3$ symmetry of the system.

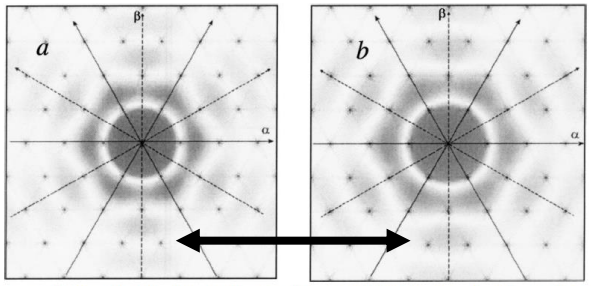

Fig. 2. a, Grid factor (regular spots) and the segment PSF_s for a perfect telescope without gaps. Except for the central peak, all peaks of the grid factor fall into zeros of the segment PSF_s. Solid and dashed arrows illustrate the same double $\pi/3$ symmetry as observed in the pupil plane (Fig. 1). b, The same, but with gaps between segments (relative gap size ω=0.1). Higher-order peaks are no longer coincident with PSF_s zeros. The same effect is seen for tip–tilt errors and segment-edge misfigure.

Figure A-1: Figures 1 and 2 from Yatiskova et al, 2003 showing aperture segmentation, ideal PSF and PSF with gaps.

For a perfectly phased telescope with no gaps and optically perfect segments, the zeros of PSF_{seg} coincide with peaks of Grid(ρ) function resulting in a smooth PSF_{tel} with a central peak size $\sim \lambda/D_{tel}$. Unfortunately, real telescopes are not perfect. Gaps between segments, segment tip/tilt errors, rolled edges and surface figure errors change the shape or redistributes energy between rings of the PSF_{seg} without changing the Grid(ρ) function.[14, 15] The effect is to produce a PSF_{tel} with energy at individual Grid(ρ) locations. This is illustrated in the right hand image of Figure A-1. A segmented aperture with tip/tilt errors is like a blazed grating removing energy from the central core into higher-order peaks. If the error is 'static' then a segmented tip/tilt deformable mirror should be able to 'correct' the error. Any residual error should be 'fixed-pattern' and thus removable from the image. But, if error is 'dynamic' (e.g. the segments are rocking), then the higher-order peaks will 'wink'.

Segment to segment co-phasing or piston errors change the Grid(ρ) function but leave the PSF_{seg} unchanged, this results in a PSF_{tel} with speckles.[14] If the error is 'static' then a segmented piston deformable mirror should be able to 'correct' the error. Any residual error should be 'fixed-pattern' and thus removable from the image. But, if the error is 'dynamic', then speckles will move in the focal plane. If the co-phasing errors are uncorrelated, then the individual speckles will add incoherently in intensity, producing an average speckle halo.[13]

APPENDIX B: TELESCOPE WFE INSTABILITY

WFE instability comes from two sources: mechanical and thermal. Mechanical vibration tends to be faster than 10 min. Thermal drift tends to be slower than 10 minutes. Thus, while a deformable mirror may correct thermal WFE drift, it cannot correct vibration. Vibration WFE must be <10 pm.

Mechanical:

Per Lake[16], rms WFE is proportional to rms magnitude of the applied inertial acceleration divided by square of the structure's first mode frequency. Therefore, to achieve <10 pm rms requires either a very stiff system or very low acceleration loads (Figure B-1, Table B-1). However, no previous space telescope has ever required <10 pm per 10-min stability. While not designed to meet the requirements of a UVOIR exoplanet science mission, JWST is an example of what is possible. The predicted response of JWST is <13 nm rms for temporal frequencies up to 70 Hz[17]. The JWST structure has an ~40 nm rms 'wing flap' mode at ~20 Hz and the individual Primary Mirror Segment Assemblies have a ~20 nm rms 'rocking' mode at ~40 Hz. To meet the exoplanet stability requirement, these amplitudes must be reduced by 1000×. JWST engineers believe that this can be done by operating at ambient with 10× more damping; making the structure stiffer; and, using active vibration isolation. JWST has ~90 dB of passive isolation. To achieve UVOIR performance requires ~140 dB of isolation.

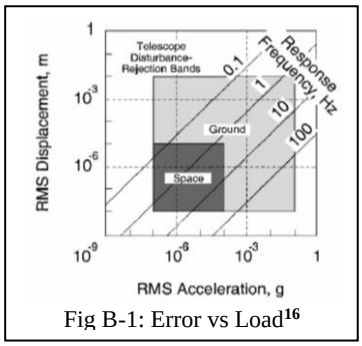

Fig B-1: Error vs Load[16]

Table B-1: WFE < 10 pm rms	
First Mode Frequency	RMS Acceleration
10 HZ	10^-9 g
100 HZ	< 10^-7 g

Thermal:

Bulk temperature stability is essential for low WFE thermal drift; however, axial and lateral gradient stability also play important roles for sub-nm WFE. When a telescope slews or rolls relative to the sun, its thermal environment changes. Heat loads to the mirror face and sides introduce axial and lateral gradients that cause WFE. These drift until the mirror reaches a new thermal equilibrium. Figure B-2 shows the typical effect of (a) bulk temperature change and (b) axial thermal flow. WFE amplitude depends on the thermal environment change and the mirror and structure's CTE (coefficient of thermal expansion). A high CTE material such as Silicon Carbide requires a more precise thermal control system than a low CTE material such as ULE® glass or Zerodur®. Table B-2 shows the thermal stability required to keep WFE <10-pm for a 16-m radius mirror. WFE drift rate depends on thermal diffusivity (conductivity/heat-capacity), boundary conditions, and whether the system has passive or active thermal control. A figure of merit for comparing mirrors is the ratio of CTE to diffusivity. Because SiC has ~100× higher thermal diffusivity than ULE® or Zerodur®, a SiC mirror will respond faster to a thermal load change and will resist thermal gradients which can change WFE. But, a SiC mirror also has ~100× higher CTE, so the ratio is similar. But, while material properties are fundamental to stability, architecture has important consequences for the control bandwidth. For low-mass space mirrors, heat transport is dominated by radiation and the high thermal diffusivity advantage of SiC is not fully realized. ULE® mirrors are typically closed-back while Zerodur® and SiC mirror are typically open-back. Open-backed mirrors have a higher thermal coupling between the facesheet and a rear heater plate that reduces settling time. Table B-3 shows the maximum bulk temperature change and axial heat flux that keeps WFE <10 pm. Even though ULE® and Zerodur® have the same CTE, the open-back Zerodur mirror is 10X less sensitive to changes in the heat flux than the ULE® mirror. The SiC substrate requires controller stability better than 1 mK/10 minutes.

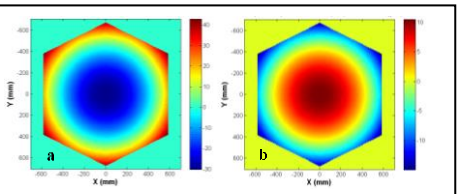

Fig B-2: WFE for a) Bulk Temp Change and b) Heat Flux

Table B-2: Thermal Stability for < 10 pm WFE		
Material	CTE	Thermal Stability
ULE® or Zerodur®	< 10 ppb	< 0.18K
SiC	< 3 ppm	< 0.0006K

Table B-3: Bulk Temperature and Axial Gradient limits for 10 pm WFE		
	ΔT (mK)	**Δ**Q (mW/m²)
ULE® 7971	140	1.7
Zerodur®	140	41
SiC	0.53	0.45

Again, no previous space telescope has ever required <10 pm per 10-min stability. Historically, space telescopes use passive thermal control. JWST is in a sun-shade shadow. HST is in a heated tube. And again, while not designed to meet the requirements of a UVOIR exoplanet science mission, JWST is predicted to have a 31 nm rms WFE response to a worst-case thermal slew of 0.22K and take 14 days to 'passively' achieve <10 pm per 10 min stability (Figure B-3)[18]. Obviously, this is too long. HST is a cold-biased telescope heated to an ambient temperature. However, it is not a controlled thermal environment. Thus, HST's WFE changes by 10–25 nm every 90 min (1–3 nm per 10 min) as it moves in and out of the Earth's shadow (Figure B-4).[19]

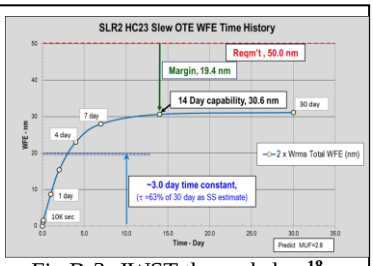

Fig B-3: JWST thermal slew[18]

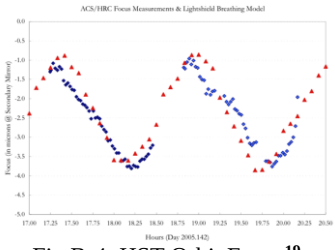

Fig B-4: HST Orbit Focus[19]

Finally, as discussed in Krist[5], one way to distinguish a planet from the background is to remove speckles by subtracting a reference PSF. This may be accomplished by rotating the telescope about the target between exposures. The instrumentally generated features (i.e. speckles) will remain stationary while the sky (including the planet) will rotate. But, this only works if the speckles remain stable to within a fraction of the planet's flux. During the ACCESS study, a detailed integrated model of a 1.5-m telescope predicted that after a 12 hour settling time from a 30 degree rotation the wavefront would have 151 picometers rms of defocus and 19 pm rms of coma and astigmatism.

ACKNOWLEDGEMENTS

This work is funded by NASA Strategic Astrophysics Technology grant NASA 10-SAT10-0048 and benefited from the critical review of Marc Postman.

BIBLIOGRAPHY

1. *New Worlds, New Horizons in Astronomy and Astrophysics*, NRC Decadal Survey, 2010.
2. *NASA Space Technology Roadmaps & Priorities*, NRC, 2012.
3. *Enduring Quests Daring Visions*, NASA, 2014
4. *From Cosmic Birth to Living Earths*, Association of Universities for Research in Astronomy, 2015.
5. Krist, John E., John T. Trauger, Stephen C. Unwin and Wesley A. Traub, "End-to-end coronagraphic modeling including a low-order wavefront sensor", SPIE Vol. 8422, 844253, 2012; doi: 10.1117/12.927143
6. Stahl, H. Philip, Marc Postman and W. Scott Smith, "Engineering specifications for large aperture UVO space telescopes derived from science requirements", Proc. SPIE 8860, 2013, DOI: 10.1117/12.2024480
7. Stahl, H. Philip Stahl; Marc Postman; Gary Mosier; W. Scott Smith; Carl Blaurock; Kong Ha; Christopher C. Stark, "AMTD: update of engineering specifications derived from science requirements for future UVOIR space telescopes", Proc. SPIE. 9143, Space Telescopes and Instrumentation 2014: Optical, Infrared, and Millimeter Wave, 91431T. (August 02, 2014) doi: 10.1117/12.2054766
8. Shaklan, "Segmented Telescope Stability Error Budget for Exo-Earth Direct Imaging", Mirror Tech Days, 2014.
9. Green, Joseph J., and Stuart B. Shaklan, "Optimizing coronagraph designs to minimize their contrast sensitivity to low-order optical aberrations", SPIE Vol.5170, pp.25, 2003.
10. Shaklan, Stuart B., Luis Marchen, John Krist, and Mayer Rud, "Stability error budget for an aggressive coronagraph on a 3.8 m telescope", SPIE Vol.8151, 815109, 2011; doi: 10.1117/12.892838
11. Lyon, Richard and Mark Clampin, "Space telescope sensitivity and controls for exoplanet imaging", Optical Engineering, Volume 51, No 1, January 2012
12. Stark, et. al., "Lower Limits on Aperture Size for an ExoEarth Detecting Coronagraphic Mission", The Astrophysical Journal, 808:149 doi:10.1088/004-637X/808/2/149, 29 July 2015.
13. Guyon, "Coronagraphic performance with segmented apertures: effect of cophasing errors and stability requirements", Private Communication, 2012.
14. Yaitskova, Dohlen and Dierickx, "Analytical study of diffraction effects in extremely large segmented telescopes", JOSA, Vol.20, No.8, Aug 2003.
15. Yaitskova and Troy, "Rolled edges and phasing of segmented telescopes", Applied Optics, Vol.50, No.4, 1 Feb 2011.
16. Lake, Peterson and Levine, "Rationale for defining Structural Requirements for Large Space Telescopes", AIAA Journal of Spacecraft and Rockets, Vol. 39, No. 5, 2002
17. Mosier, Gary, "Isolation Requirement", AMTD Report, 2014
18. 13-JWST-0207 F, 2013
19. Lallo 2012, Opt. Eng. Vol. 51, 011011, January 2012 doi: 10.1117/1.OE.51.1.011011
20. Sivaramakrishnan, et al., "Ground-based coronagraphy with high-order adaptive optics", The Astrophysical Journal, 552:397-408, 2001 May 1
21. Soummer, et. al., "Fast computation of Lyot-style coronagraph propagation", Optical Society of America, 2007.
22. Kuchner, Marc J. and Wesley A. Traub, "A coronagraph with a band-limited mask for finding terrestrial planets", The Astrophysical Journal, 570:900-908, 2002 May 10